Front. Mater. Sci. 2021, 15(3): 374–390
https://doi.org/10.1007/s11706-021-0568-2

REVIEW ARTICLE

Metal-organic framework-based intelligent drug delivery systems for cancer theranostic: A review

Qingni XU, Chaohua LI, Yuqi CHEN, Yueli ZHANG, and Bo LU (✉)

School of Chemistry, Chemical Engineering and Life Sciences, Wuhan University of Technology, Wuhan 430070, China

ABSTRACT: The design and development of multifunctional nano-drug delivery systems (NDDSs) is a solution that is expected to solve some intractable problems in traditional cancer treatment. In particular, metal-organic frameworks (MOFs) are novel hybrid porous nanomaterials which are constructed by the coordination of metal cations or clusters and organic bridging ligands. Benefiting from their intrinsic superior properties, MOFs have captivated intensive attentions in drug release and cancer theranostic. Based on what has been achieved about MOF-based DDSs in recent years, this review introduces different stimuli-responsive mechanisms of them and their applications in cancer diagnosis and treatment systematically. Moreover, the existing challenges and future opportunities in this field are summarized. By realizing industrial production and paying attention to biosafety, their clinical applications will be enriched.

KEYWORDS: metal-organic framework; nanomaterial; stimuli-responsiveness; cancer theranostic

Contents

Received June 23, 2021; accepted August 12, 2021

E-mail: lvb@whut.edu.cn

1 Introduction

Every year, millions of people die of cancer, which is the second leading cause of death for mankind [1–2]. Cancer has become a pressing global public issue and the focus of major research worldwide. Chemotherapy is a traditional mode of cancer treatment, in which the delivery method of drugs is a crucial factor that affects the therapeutic effects of drug molecules. Because traditional chemotherapy drugs cannot distinguish tumor cells from normal cells, they have limitations such as nonspecific toxicity, poor tumor aggregation, easy drug resistance, and fast blood clearance rate [3–7]. Therefore, in addition to the development of

effective chemical drugs, the construction of effective nanocarriers is also very important for the optimization of chemotherapy, which has become a research hotspot [8–10].

With the development of nanotechnology and the higher expectation on the effect of tumor therapy, scientists have made a lot of efforts to establish nanomedicine delivery system to meet different needs, resulting in the rapid development of nanoparticulate drug delivery systems (DDSs) [11]. Currently, the nanoparticulate DDSs developed and researched are mainly divided into two categories: one is inorganic nanoparticulate DDS (such as gold nanoparticles (NPs) [12–13], Fe_3O_4 NPs [14–16], nano-mesoporous silicon [17–19], and carbon nanomaterials [20–22]); the other is organic nanoparticulate DDS (such as liposomes [23–25], polymer micelles [26–28], and nano-albumin [29]). Inorganic materials have certain generality, such as stability, inertia, optics and magnetism, but they are not easily degraded and are easy to accumulate in the body [30]. The difference is that the organic materials are easy to modify, and have good biocompatibility and low toxicity, but their purity and drug loading capacity are insufficient.

Metal-organic frameworks (MOFs), a class of porous materials based on metal ions and organic linkers, have shown unique properties including high porosity, large surface area, tunable pore size and abundant metal/organic ligands design [31]. Due to their unique structures and properties, MOFs have been widely used in the fields of gas storage, material separation and catalysis [32–34], and show significant potential in nanomedicine in cancer theranostic [35–36]. As a DDS, MOFs should meet the following requirements: (i) Low toxicity. Biosafe metal and organic linkers are selected to synthesize to ensure their biological safety [37]. (ii) The particle size is less than 200 nm, which has a higher cell uptake rate, a longer blood circulation time and the effect of enhanced permeability and retention (EPR) of drug concentration in the tumor region [36]. (iii) Large specific surface area and high porosity. This makes possible higher drug loading capacity [38]. (iv) Surfaces can be modified [39–40]. Stability and surface properties are strictly required. (v) Biodegradability. This allows them to degrade rapidly after the expected task is completed and to be excreted from the body, preventing endogenous accumulation and associated toxic effects [41]. Moreover, the effective accumulation of MOFs at the tumor site to release loaded drugs in the complex tumor microenvironment is a major challenge for their biomedical applications. To meet this challenge, various stimulus types (such as pH, glutathione (GSH), adenosine triphosphate (ATP), and light) and targeted MOF-based DDSs have been reported, enriching the approach for tumor theranostic [42–43].

Here, we give an overview of the recent research progress and future development of MOFs in biomedical applications, particularly focusing on the practical applications of MOFs as nanoparticulate DDSs for cancer theranostic.

2 MOF-based stimuli-responsive DDSs

Stimulus-responsive MOFs, also known as smart MOFs, refer to the fact that after the introduction of stimulus-responsive groups or materials, the smart materials will undergo conformational changes, protonation or hydrolytic cleavage under endogenous and/or exogenous stimulus, resulting in the release of guest molecules. Among them, endogenous stimulation mainly includes pH [11,38], redox activity [44–45], biomolecules [46–47], etc., while exogenous stimulation mainly includes light [48–50], magnetic field [51–52], ultrasonic wave [53], etc. In the process of blood circulation and infiltration of drug-loaded NPs into the tumor stroma, drugs may leak ahead of time, resulting in insufficient drug concentration in the tumor site, thus reducing the therapeutic effect and causing toxic and side effects. To overcome this obstacle, a series of smart MOFs have been designed. In this section, endogenous stimulus-responsive and exogenous stimuli-responsive MOF-based DDSs will be discussed, respectively.

2.1 Endogenous stimulus-responsive MOF-based DDSs

2.1.1 pH-responsive drug release

Among many endogenous stimulus responses, the pH response is one of the most widely investigated controlled release mechanisms of anticancer drugs. The pH of the infection, the primary tumor, and the site of the metastatic tumor are all lower than those of the normal tissue because tumor cells produce large amounts of lactic acid (LA) when they degrade glucose, and the acidic organelles within the cell are more acidic (endosomes and lysosomes) [54–55]. Many acid-sensitive MOFs (such as ZIF-n, MIL-n, and UiO-n), acid-labile bonds (such as amide bonds, Schiff base bonds, and boronate ester bonds) or other pH-sensitive materials (such as carboxymethyl cellulose

(CMC), chitosan, and gelatin polymers) can be destroyed at low pH, resulting in the release of payload [11,56]. Zeolitic imidazolate framework-8 (ZIF-8) is stable at pH 7.4 and decompositions under acidic conditions because the coordination between zinc and imidazolate ions decompositions at pH 5.0–6.0. With the release of large amounts of Zn^{2+}, it could be synergistic in promoting tumor chemotherapy, which has been demonstrated by Jiang and colleagues [57]. Sun et al. selected ZIF-8 as the drug carrier, loaded D-α-tocopherol succinate (α-TOS), and finally covered the surface of ZIF-8 with a layer of hyaluronic acid (HA) through the electrostatic interaction between Zn^{2+} and COO^- in HA to form HA/α-TOS@ZIF-8 NPs [42]. HA is a natural polysaccharide, which is abundant in extracellular matrix and has good biocompatibility, non-toxicity and biodegradability. In this drug delivery system, the HA shell not only has CD44-targeting effect to actively target breast cancer cells [58], but also can be used as an intelligent response "switch". When the NPs are targeted to the tumor region, the electrostatic interaction between Zn^{2+} and COO^- decreases due to increased acidity, resulting in the detachment and biodegradation of the HA shell by hyaluronidase. After that, the naked α-TOS@ZIF-8 will rapidly degrade under acidic conditions, and then release α-TOS to achieve tumor chemotherapy. High inhibiting tumor growth performance *in vivo* and *in vitro* revealed that the as-developed HA/α-TOS@ZIF-8 nanoplatform had the potential in tumor-specific and on-demand drug clinical practice (Fig. 1) [42]. Li's team also used ZIF-8 to prepare a pH-responsive DDS [59]. The difference is that they integrate Gd-doped silicon nanoparticles (Si–Gd NPs), chlorine e6 (Ce6), doxorubicin (DOX), ZIF-8, poly(2-(diethylamino) ethyl methacrylate) polymer (HOOC-PDMAEMA-SH) and folic acid–poly (ethylene glycol)–maleimide (MaL–PEG–FA) into one single nanoplatform through the self-assembly method. The polymer (HOOC-PDMAEMA-SH) has a pK_a of 7.3, and swells under acidic pH conditions, so it can be used to achieve drug release through pH response in a tumor microenvironment [60]. These pH-responsive MOFs have shown superior therapeutic efficacy in tumors. However, the bioavailability and response rate of these MOFs to pH stimulus require attention to adapt to appropriate applications.

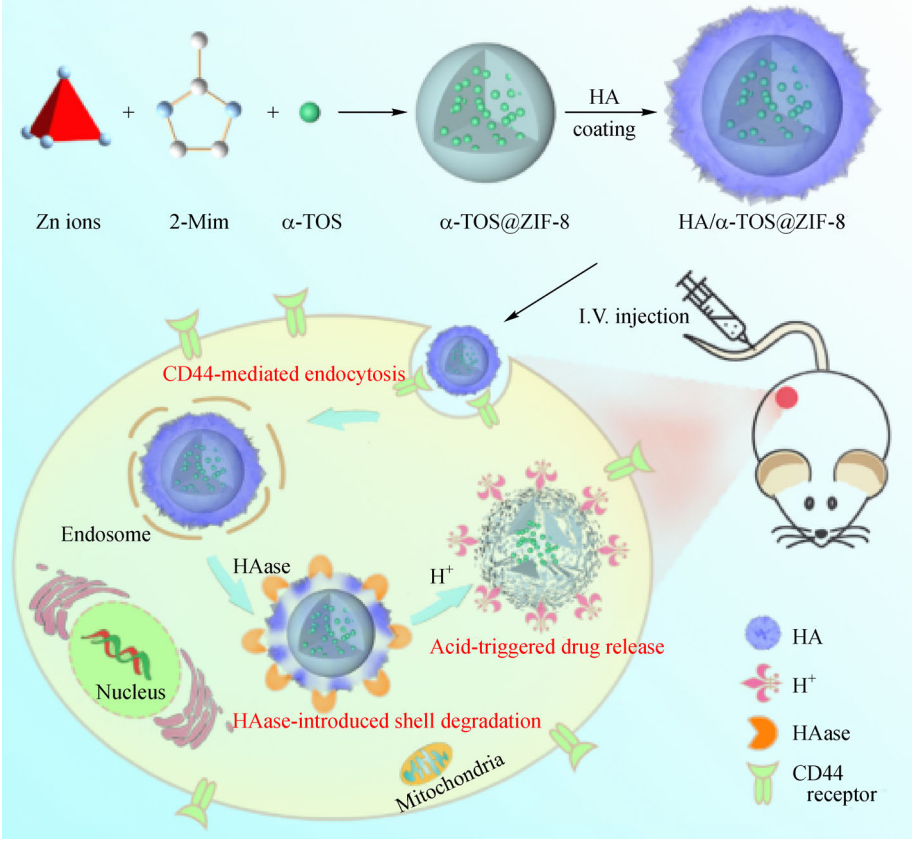

Fig. 1 Schematic illustration for the formation and drug release mechanism of the HA/α-TOS@ZIF-8 nanoplatform. Reproduced with permission from Ref. [42].

2.1.2 GSH-responsive release

The significant difference in redox potentials between intracellular and extracellular environments is also commonly used as the stimulus for DDSs. Compared to normal tissues, high GSH concentration (from 2 to 10 mmol·L^{-1} in the cytoplasm) is a major feature of tumor tissues, which is 100–1000 times higher than that in blood and extracellular matrix (2 μmol·L^{-1}) [61–62]. More importantly, GSH is a strong reducing agent that can be oxidized by oxidizing substances such as disulfide bonds [63]. The design of disulfide bonds mainly includes introducing organic ligands containing disulfide bonds and modifying molecules containing disulfide bonds on the MOFs surface. Among them, introducing organic ligands containing disulfide bonds is the most direct method for the preparation of GSH-responsive DDSs. Lei et al. incorporated organic ligands containing disulfide bonds as linkers within the structure of a MOF [64]. They prepared the intrinsic redox-responsive MOFs with iron, aluminum or zirconium as the metal node, 4,4′-dithiobenzoic acid (4,4′-DTBA) as the GSH-sensitive organic compound system. In these MOFs, they chose MOF-Zr(DTBA) as the carrier of curcumin (CCM), and subsequently obtained CCM@MOF-Zr(DTBA) NPs that displayed a faster releasing behavior *in vitro* and enhanced the cell death compared with free CCM (Fig. 2). Similarly, Jiang et al. created a novel tumor-sensitive biological MOF (bioMOF-Zn(Cys)) through the assembly of endogenous Zn^{2+} ions and the small biological molecule L-cystine (Cys) [43]. The disulfide bond in Cys is cleavable by the overexpressed GSH in tumor cells, thus achieving rapid release of drugs from nanocarriers. By encapsulating DOX in bioMOF-Zn(Cys), DOX@bioMOF-Zn(Cys) displayed higher cellular uptake and cytotoxicity in cancer cells than free DOX. *In vivo* investigations indicated that DOX@bioMOF-Zn(Cys) largely inhibited tumor growth and reduced side effects. As a matter of fact, the latter approach is easier to implement than the former strategy. In the presence of GSH, the binder or surface coating breaks down rather than the structure of the MOFs. Liu et al. obtained Zr-MOF coated with a disulfide bonded polymer (poly(N,N'-bis(acryloyl)cystamine) (PAC)) by *in situ* polymerization on the Zr-MOF surface [65], which gave the NPs (Zr-MOF-PAC) strong physiological stability and the ability to release drugs in response to the GSH stimuli. The polymer coating on the surface can prevent the decomposition of Zr-MOF in phosphate medium or acid environment, and prevent drug leakage. This method effectively solved the problem that the instability of traditional Zr-MOF in phosphate medium caused drug leakage under physiological conditions. Therefore, this strategy can not only improve the physiological stability of Zr-MOF but also promote the release of stimulus-responsive drugs. Based on this strategy, Zr-MOF is one step closer to further clinical research on the application of tumor treatment via intravenous injection. In the future, in addition to continuously exploring new types of MOF-based DDSs, the optimization of existing MOF-based DDSs also needs to be encouraged.

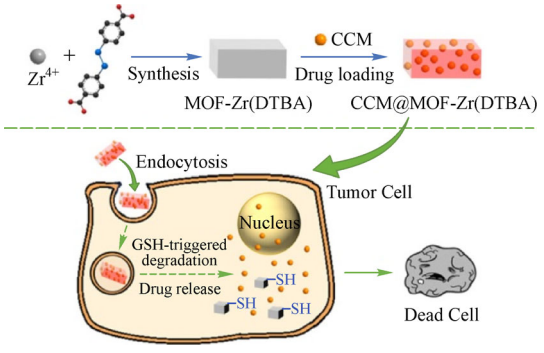

Fig. 2 Schematic illustration of the preparation of CCM@MOF-M(DTBA), and the redox-responsive degradation of CCM@MOF-M(DTBA) in tumor cells for cancer therapy. Reproduced with permission from Ref. [64].

2.1.3 ATP-responsive release

ATP is a very important organic compound, which exists widely in organisms and has strong coordination ability. ATP is overexpressed in tumor cells. Because ATP can form ATP aptamer complexes with DNA/RNA and can also coordinate with metal ions, ATP can be used as a drug-controlled release factor in MOF-based DDSs [66–68]. Chen et al. loaded DOX with MOF NPs and coated it with a polyacrylamide/DNA hydrogel that can stimulate response [69]. The crosslinking of this hydrogel is achieved in a cage structure by means of a nucleic acid double-stranded body containing an anti-ATP aptamer. In the presence of ATP, this cross-linked bridging unit is separated by the formation of the ATP–aptamer complexes, which leads to the separation of the hydrogel shell and the release of the drug. In view of strong coordination of phosphate and metal ions, Wan et al. prepared an ATP-regulated ion transport nanosystem (SQU@PCN) by encapsulating the squaramide (SQU) in porphyrinic porous coordination network (PCN) [70]. The highly expressed ATP in the tumor can coordinate with the metal in SQU@PCN, resulting in the disintegration of the

nano-transporter and the release of SQU contained in the nano-transporter. It is interesting to note that this work demonstrates that SQU can mediate chloride ion influx and H^+/Cl^- coupled transporter to induce apoptosis and autophagy inhibition in tumor cells (Fig. 3). Therefore, such a strategy of synergistic treatment between PCN-based photodynamic therapy and SQU-based homeostatic perturbation therapy showed outstanding *in situ* tumor eradication while blocking the metastasis from the source, which offers a promising approach to cancer therapy using functional compounds rather than traditional chemotherapy drugs.

2.2 Exogenous stimuli-responsive MOF-based DDSs

2.2.1 Light-responsive release

It is known that the superiority of light-responsive DDSs lies in their non-damage characteristics and the flexibility that can be accurately controlled remotely [71]. And they can precisely control the release time and location of the drug by changing the light intensity, time, location, and wavelength [72–74]. The two most common light-responsive drug release pathways are drug release based on photochemical and photothermal mechanisms. Among them, the photochemical drug release system usually contains some photosensitive groups or photosensitizers (PSs). Nanoscale porphyrinic MOFs, regarded as one of the fourth generation of PSs, have shown great potential in tumor treatment since the first light-responsive MOF was used in the treatment of tumors in 2014 [75–76]. Li et al. prepared ultrathin copper-tetrakis(4-carboxyphenyl)porphyrin (Cu-TCPP) MOF nanosheets by a facile solvothermal route. Due to the inherent characteristics of TCPP, Cu-TCPP has the ability to produce singlet oxygen after irradiation by near-infrared (NIR) light, which has a strong killing effect on tumor cells [77–78]. Compared with the PSs not wrapped by NPs, the PSs wrapped by NPs can have a higher degree of enrichment in the body and have better pharmacokinetics. Researchers are gradually combining the benefits of MOFs and molecular targeted therapies to achieve favorable therapeutic outcomes. Wang et al. reported a ZIF-8-assisted *in vivo* self-assembled nanoplatform loaded PSs, poly(methyl methacrylate) (PMMA) and disulfide-linked methoxy polyethylene glycol (S-S-mPEG) coupled ZIF-8 (PS@ZIF-8-PMMA-S-S-mPEG) [79]. Under intratumoral bioreduction, PS@ZIF-8-PMMA-S-S-mPEG was self-assembled into large ordered hydrophobic clusters, which greatly enhance tumor retention and accumulation of the PSs. Therefore, this strategy realized maximized intratumoral $^1O_2$ photosensitization of loaded organic PSs under light irradiation. In another study, Yang et al. prepared MIL-100 coated upconversion nanoparticles (UCNPs) using a one-pot process [80]. The encapsulation of UCNPs into MIL-100(Fe) shell leads to core–shell structured UCNPs@MIL-100(Fe) NPs. The porous structure and high specific area of the MOFs shell enable it possible to load large amount of toxic DOX.

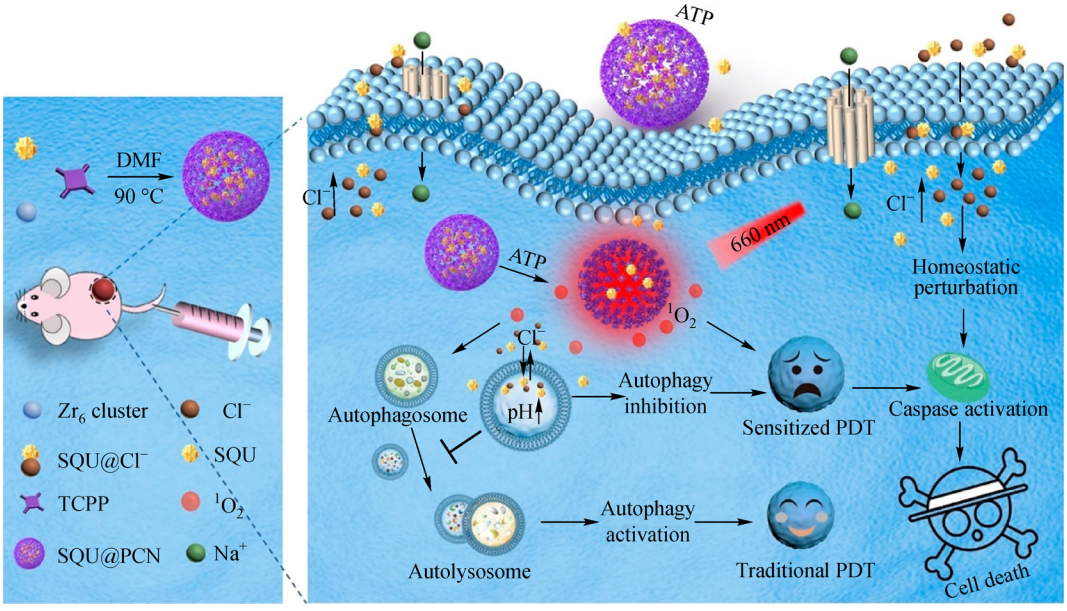

Fig. 3 Schematic illustration of SQU@PCN preparation and the tumor cell death process by homeostatic perturbation therapy and sensitized photodynamic therapy. Reproduced with permission from Ref. [70].

Under the irradiation of NIR light, NPs can convert light energy into heat energy to realize photothermal therapy (PTT). At the same time, due to the rise of temperature, the release amount of DOX is greatly increased (Fig. 4). Nowadays, many MOF-based DDSs that combine light response with endogenous response have enriched their cancer treatment applications (such as NIR light/pH and NIR light/GSH [81–82]), and future research should focus on improving the loading efficiency, biocompatibility and biodegradability of them.

2.2.2 Ultrasound-responsive release

Existing diagnostic and treatment technologies of ultrasound, such as B-type ultrasound and kidney stone breakage, have proven the safety and biological tolerance of such technology [83]. Ultrasound can act as an effective stimulus mode for DDSs because of its non-invasive, non-ionizing radiation and deep tissue penetration [84]. Ibrahim et al. used iron-based MOF (namely, Fe-NDC) as a carrier to load calcein and DOX [85]. *In vitro* release experiments have shown that when ultrasound is used, the release of DOX reached 80% after 254 min, while in the absence of ultrasound, it only reached 6%. It shows that the system has good ultrasonic response capabilities. In recent years, sonodynamic therapy (SDT) has developed rapidly as a new type of cancer therapy. SDT kills tumor cells by producing reactive oxygen species (ROS) through the participation of sound sensitizer and oxygen under the action of ultrasonic radiation [86–87]. Pan et al. prepared MOFs-derived double-layer hollow manganese silicate (DHMS) NPs, which were synthesized by *in-situ* growth of Mn^{2+} with ZIF-8 as template [88]. The transition metal element Mn can be oxidized by holes under ultrasound radiation, which effectively improves the electron–hole separation. Therefore, DHMS can produce a large number of singlet oxygen and hydroxyl radicals under ultrasound radiation. In addition, DHMS NPs have the excellent ability to produce O_2 by reacting with endogenous H_2O_2, which can overcome tumor hypoxia to improve the efficiency of SDT (Fig. 5). This study proposed MOFs-derived NPs with sound sensitivity and oxygen production ability, which provides a promising strategy for tumor hypoxia in SDT.

2.2.3 Magnetic-responsive release

Compared with other controlled release methods, magnetic field has a strong ability to penetrate organisms and has no adverse effects on biological tissues [89]. In general, MOF-based DDSs with magnetic field response usually contain components such as magnetite (Fe_3O_4) or maghemite

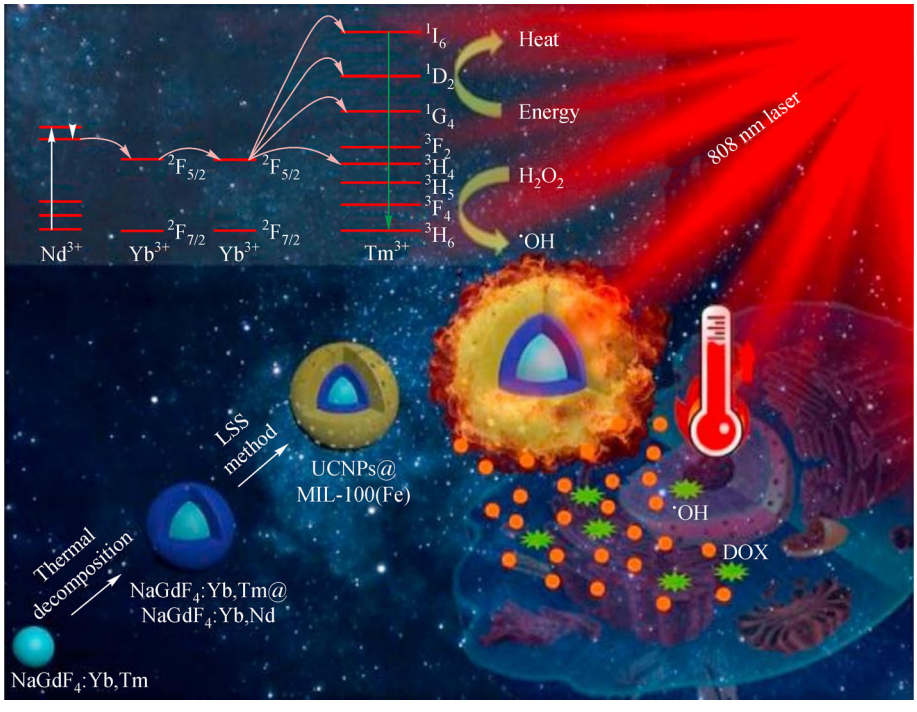

Fig. 4 Schematic illustration for the formation and drug release mechanism of UCNPs@MIL-100(Fe) NPs. Reproduced with permission from Ref. [80].

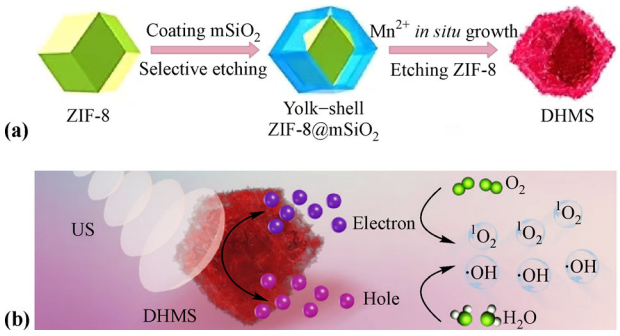

Fig. 5 **(a)** Scheme of the synthesis process for DHMS. **(b)** The proposed mechanism of ROS generation by DHMS under ultrasound irradiation. Reproduced with permission from Ref. [88].

(Fe_2O_3), which gather at the target under the action of magnetic fields to release drugs for therapeutic effect, or use magnetic fields to heat magnetic cores to increase local temperature and control drug release [90]. Xiang et al. reported a novel porous Fe_3O_4@C–PVP@DOX nanocomposite derived from MOF, in which Fe_3O_4@C was obtained by high temperature decomposition of Fe-MOF. Under the action of alternating magnetic field, Fe_3O_4@C–PVP@DOX nanocomposite material can increase the temperature of the tumor site and release DOX on demand, resulting in the death of tumor cells [91]. *In vivo* animal experiments have confirmed that the system can significantly inhibit the growth of malignant tumors, and the side effects are negligible (Fig. 6). Notably, magnetic MOFs also have the capability of magnetic resonance imaging (MRI), and are widely studied as MRI-guided diagnostic systems at present. This application will be discussed in a subsequent section and some recent examples will be provided.

3 MOF-based targeted DDSs

Targeted drug delivery system by selectively concentrating drugs on the target site plays a vital role in the mitigation of adverse effects that are raised in cancer [92]. Generally speaking, there are three ways for drugs to target tumor cells, namely passive targeting, active targeting and homotypic targeting. Compared with normal tissues, tumor tissues have wider gaps in blood vessel walls and lack of lymphatic reflux, causing macromolecules and nanoparticles (usually between 30 and 200 nm) to gather in them [93–94]. Owing to this so-called EPR effect, MOFs with adjustable particle size can achieve passive targeting. However, it is not enough to rely on passive targeting alone to achieve precise cancer treatment, so researchers will want to focus on developing more targeting methods to achieve this goal.

To enhance the uptake of MOFs in tumor cells, MOFs have been conjugated with diverse array of targeting ligands, which have specific affinity to the receptors over-expressed on the surface of cancer cells, including HA [95–96], FA [97–98], lactobionic acid [99–100], arginine-

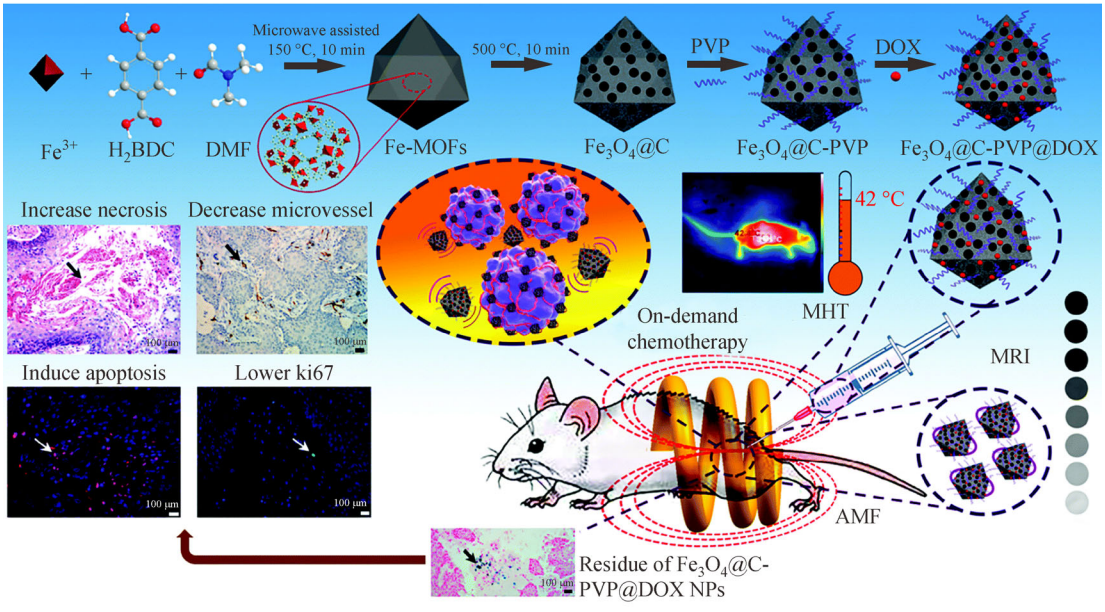

Fig. 6 Schematic illustration of the design and application of novel porous Fe_3O_4@C–PVP@DOX nanocomposites as smart platforms for the combined cancer therapy. Reproduced with permission from Ref. [91].

glycine-aspartate (RGD) [101] and others. The successful specific drug delivery to cancer cells was reported by Zhang and coworkers [102]. They encapsulated glucose oxidase (GOx) in MIL-100 and coated NPs with polydopamine-modified hyaluronic acid (HA-PDA) to construct a novel positive feedback nano-amplifier with self-enhancing tumor therapeutic capabilities. In another study, the tumor suppression *in vivo* was also greatly improved by HA-modified MOFs [103]. Yan et al. synthesized FA-conjugated ZIF-8 by a facile amidation reaction and loaded DOX prodrug (CAD@ZIF-8) [97]. The cellular uptake study indicated that the CAD@ZIF-8–FA NPs showed significantly higher uptake in the MDA-MB-231 cancer cells, which was induced by folic-mediated endocytosis.

In recent years, a growing number of studies have wrapped cancer cell membranes from different sources on the surface of nanomaterials to endow nanomaterials with the ability of immune escape and homologous recognition and targeting [104]. This is mainly due to the fact that most of the target molecules of cancer cells can recognize cancer cells through the specific ligand-receptor interaction between the overexpressed antigens on the surface of the cancer cell membrane [105]. Wan et al. designed a 4T1 cell membrane-cloaked cascade nanoreactor based on MIL-100 and GOx decoration for synergistic ferroptosis-starvation anticancer therapy (Fig. 7) [106]. The experimental results show that the cancer cell membrane endows the nanoreactor homologous targeting and immune escaping ability, which facilitated the nanoreactor to accumulate into tumor site with high efficiency. The mechanism of this targeted therapy that makes full use of the mutual affinity between cancer cells allows more researchers to understand the advantages of MOFs in the treatment of cancer.

4 Multifunctional MOF-based theranostic nanosystems

As individual differences will directly affect the effect of tumor treatment, the development of individualized

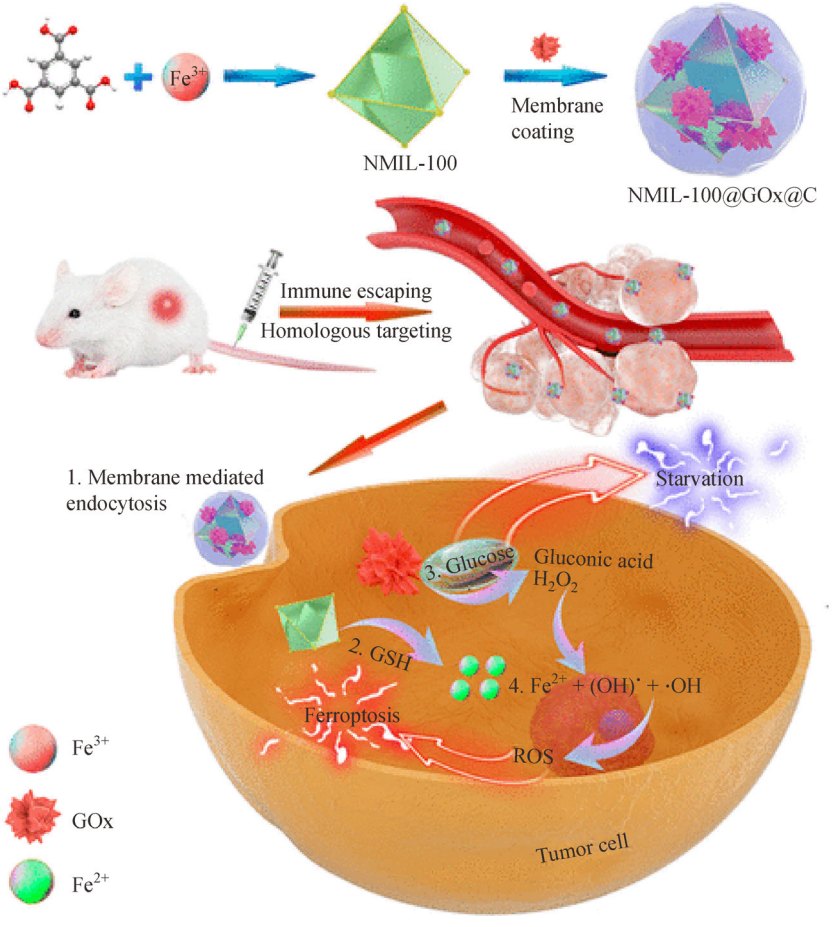

Fig. 7 Schematic illustration of the preparation of NMIL-100@GOx@C and the cascade processes for cancer therapy. Reproduced with permission from Ref. [106].

theranostic nanosystems is the development trend of tumor treatment in the present, the system is able to integrate different diagnoses and treatments in a system that can real-time monitoring *in situ* in the presence of drugs in the body to absorb, distribution, metabolism, and evaluate the effect of the treatment in a timely manner [107–110]. Due to the rapid progress in the study of MOFs and their advantages and great potential, MOFs have been widely used in medical imaging and *in situ* diagnosis [36,111–113]. In this section, we will discuss the various applications of MOFs in cancer theranostic.

Biomedical imaging is an important method for cancer diagnosis, which can be used for cancer detection, screening and diagnosis. Through diagnosis, it can be judged whether cancer has occurred, and information such as its size, location, and marginal boundaries can be obtained. There are many imaging modes for MOF-based theranostic nanosystems, such as MRI [114], computed tomography (CT), fluorescence imaging (FI), photoacoustic imaging (PAI), etc. Researchers usually design MOF-based theranostic nanosystems with different functions for their intended purposes. For example, paramagnetic ions (such as Gd^{3+} [115] and Mn^{2+} [116]) doped in MOFs can be used as the T_1 contrast agent for MRI, or magnetic Fe_3O_4 NPs can be used as nuclei to prepare magnetic nanoparticle@MOF NPs with the shell–nucleus structure to realize the T_1/T_2 dual-mode MRI [117]. Zhou et al. doped MnO_x into MOF formed by zirconium chloride, tetrafluoro-terephthalic acid and phosphate-PEG (PPEG) on their surface (MnO_x/UiO-66-F/PPEG) [118]. MnO_x/UIO-66-F/PPEG NPs would collapse in a weak acidic tumor microenvironment, releasing MnO_x and free F_4PTA. Although the content of ^{19}F nucleus in the body itself is very low (except bones and teeth), it can be detected by MRI with high penetration depth and low background noise due to the presence of free F_4PTA [119]. Then MnO_x can be reduced to Mn^{2+} under the action of GSH overexpressed in tumor microenvironment, which enables NPs to have the T_1-weighted MRI function (Fig. 8).

In recent years, PAI, which produces images in the form of ultrasonic wave by means of laser pulse and receiving sound information, has developed rapidly as a non-invasive medical imaging method and has broad application prospects in physiological and pathological visualization. Zhu et al. constructed DOX/Pd@ZIF-8 by means of self-assembly, in which Pd nanosheets and DOX were encapsulated in ZIF-8. In order to prevent premature drug leakage and make the NPs more versatile, PDA was coated

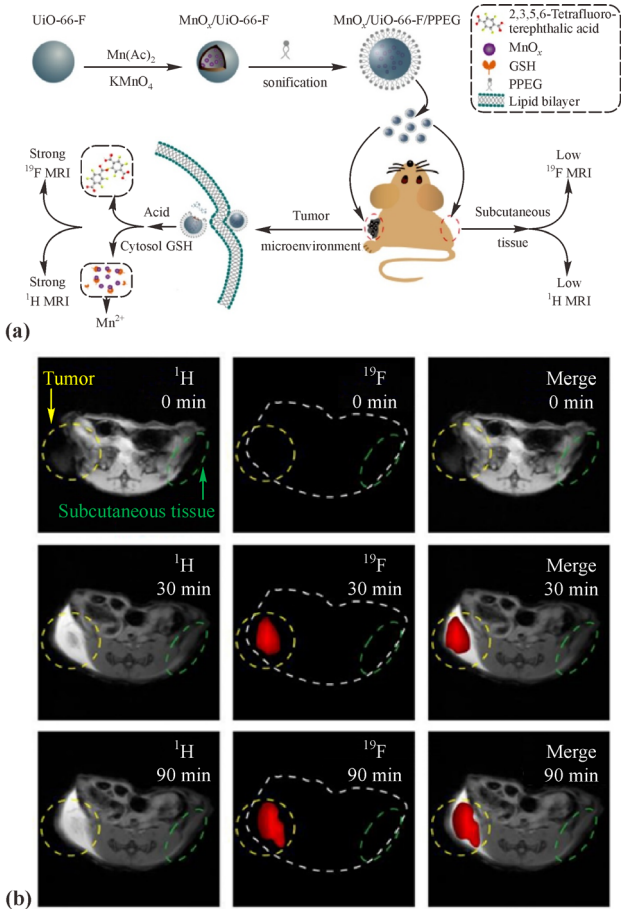

Fig. 8 **(a)** Synthesis of MnO_x/UiO-66-F/PPEG NPs and $^1H/^{19}F$ dual-mode imaging of MnO_x/UiO-66-F/PPEG NPs *in vivo*. **(b)** The representative ^1H MRI, ^{19}F MRI, and the merge of ^1H MRI and ^{19}F MRI under a 7 T magnetic field at different time (0, 30 and 90 min, respectively) in tumor and subcutaneous tissue with a dose of 249.4 mg·kg^{-1} body weight. Reproduced with permission from Ref. [118].

on the surface of the particles (DOX/Pd@ZIF-8@PDA) [120]. *In vitro* drug release studies have shown that DOX released in a pH-dependent manner. However, due to the photothermal effect of Pd nanosheets and PDA, drug burst release can be achieved in a relatively short time under 808 nm NIR light irradiation. In addition, the PAI capability of DOX/Pd@ZIF-8@PDA is activated (Fig. 9). *In vitro* and *in vivo* studies have shown that this dual stimulus response guided by PAI, in conjunction with photo-chemical cancer therapy, can effectively eliminate tumors.

Although each imaging method has its own outstanding advantages, at the same time, due to background tissue noise, tissue metabolism and limited resolution and signal penetration ability, a single imaging technique lacks specificity and sensitivity, which makes it unable to meet

the growing practical needs. Hence, in order to solve the problem of insufficient single mode imaging, multi-mode imaging system which can provide comprehensive and accurate diagnostic information with high sensitivity, real-time and high temporal and spatial resolution has become a research hotspot [121]. Wan et al. designed and constructed Mn^{3+}-sealed MOFs using a one-pot method through the chemical coordination of Mn^{3+} and TCPP (Fig. 10(a)) [122]. As a sealing agent, Mn^{3+} can not only quench the fluorescence of TCPP, but also inhibit the production of ROS, which make MOFs "inert" diagnostic NPs. Interestingly, after endocytosis by tumor cells, MOFs were decomposable by GSH in tumor cells into Mn^{2+} and free TCPP due to the redox reaction between Mn^{3+} and GSH. MRI of Mn^{2+} combined with FI of TCPP facilitates the visualization of the NPs (Figs. 10(b)–10(e)). More importantly, this GSH-regulated release of TCPP enables controlled release of ROS under light, avoiding side effects (inflammation and damage to normal tissues). Therefore, Mn^{3+}-sealed MOFs can perform precise dual-mode tumor localization and increase the treatment efficiency of photodynamic therapy (PDT). More recently, Zhu et al. prepared Fe-DOX NPs by poor solvent precipitation method, and then coated them with MOFs formed by Gd^{3+} and 1,3,5-benzoic acid (H_3BTC) ligand, obtaining Fe-DOX@Gd-MOF nanoparticles (FDG NPs) [123]. With the protection of Gd-MOF shell, FDG NPs could effectively concentrate on tumor sites and release DOX through pH response. At the same time, with a high γ_2 relaxivity, Gd-MOF provided material with potential application for MRI. Furthermore, the photoresponsive indocyanine green (ICG), the only NIR organic dye for

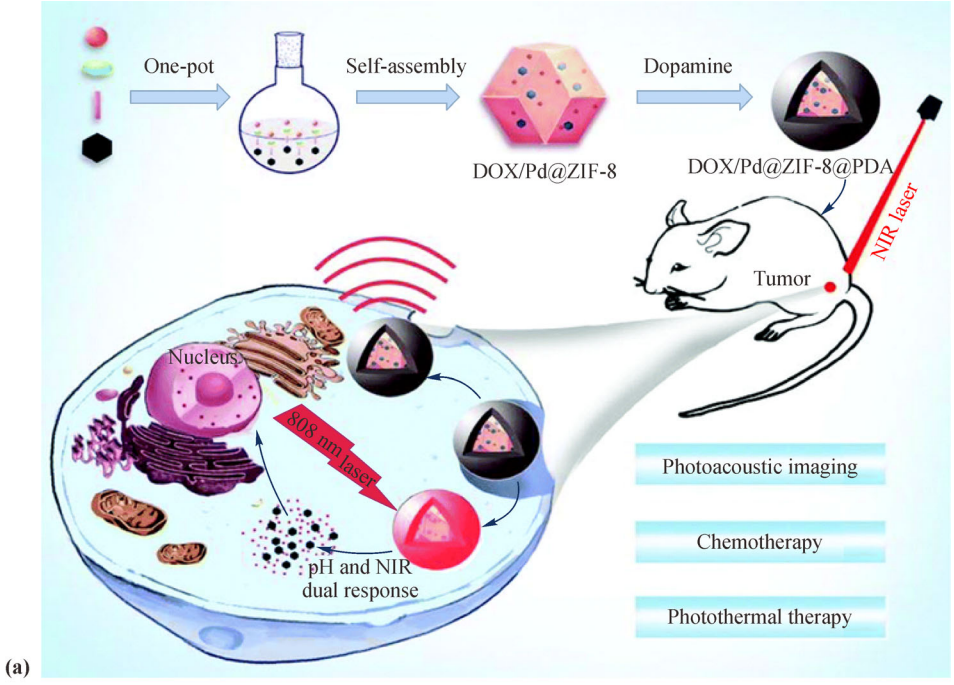

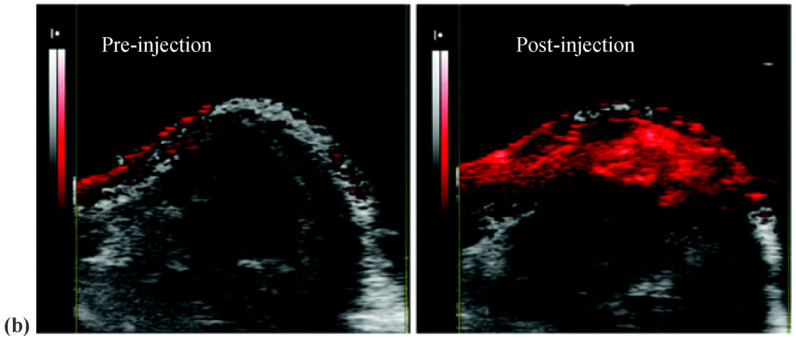

Fig. 9 **(a)** Schematic illustration of the design and application of DOX/Pd@ZIF-8@PDA NPs. **(b)** PA imaging of DOX/Pd@ZIF-8@PDA NPs in tumor site. Reproduced with permission from Ref. [120].

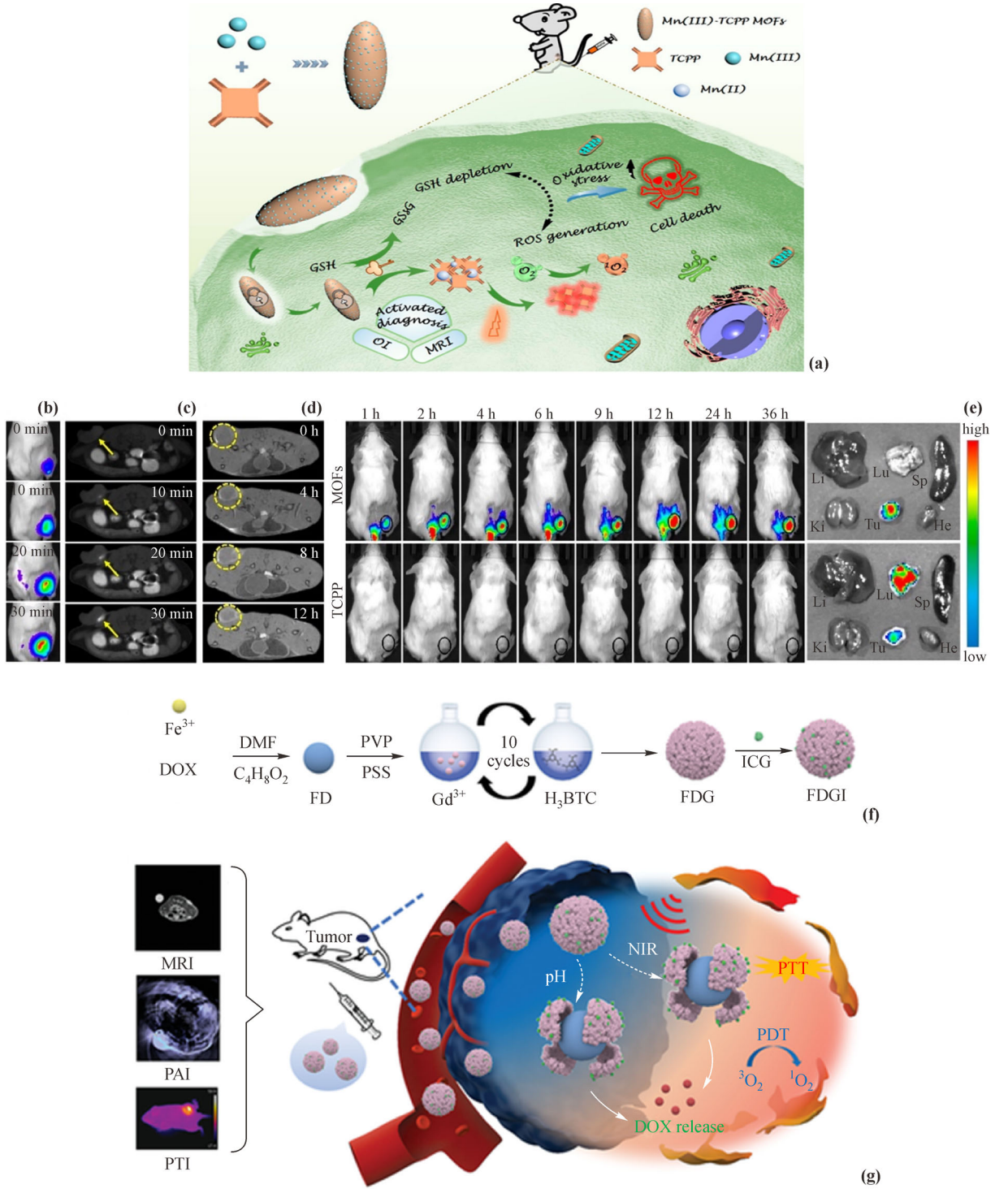

Fig. 10 **(a)** Schematic illustration of an endocytosis Mn^{3+}-sealed MOF nanosystem for MRI- and OI-guided PDT by controlled ROS generation and GSH depletion after being unlocked by overexpressed GSH in tumor cells. **(b)** Fluorescence and **(c)** T_1 contrast signals in tumor sites by intratumoral injection within 30 min. **(d)** *In vivo* MRI signal after intravenous injection with MOFs. **(e)** FI of mice over time by intravenous injection and tissue imaging at 36 h postinjection [122]. **(f)** Schematic illustration of the fabrication process of FDGI NPs. **(g)** Schematic illustration of FDGI theranostic nanoplatform for MR/PA/PT imaging-guided chemotherapy, PTT and PDT compound antitumor therapy [123]. Reproduced with permission from Refs. [122–123].

clinical applications approved by the FDA [71,124–125], was loaded into the FDG NPs to fabricate Fe-DOX@Gd-MOF–ICG nanoparticles (FDGI NPs) for PTT/PDT combination therapy guided by PAI/photothermal imaging (PTI). *In vitro* and *in vivo* experimental results showed that FDGI NPs exhibited excellent T_2-weighted MRI, PAI and PTI capabilities, and effectively inhibited 4T1 cells through combined chemo-phototherapy (Figs. 10(f) and 10(g)). Therefore, such MOF-based theranostic nanoplatform represents a new system for multimodal imaging technology to guide combined anti-tumor therapy, and provides a new idea for the design of multi-functional MOF structure for tumor treatment.

5 Conclusions and future perspective

In the present review, the MOFs potential to be used as intelligent theranostic nanosystems was highlighted. These systems have excellent features such as high drug loads, controlled cargo release, and integrated diagnosis and treatment, so they can avoid premature drug degradation, increase drug concentration at tumor sites, avoid drug interaction with normal tissues, and ultimately improve drug bioavailability and therapeutic effect. The strategies employed by the researchers to obtain stimulus-responsive theranostic systems from MOFs include surface coating or functionalization, and internally loaded functional compounds, making them promising candidates as DDSs for cancer theranostic.

Despite recent extensive research on the development of MOF-based theranostic nanosystems for cancer, most of them are still in the laboratory research stage. It is necessary to develop MOF-based DDSs that meet the requirements of industrial production to facilitate their development as clinical theranostic agents. In addition, the biosafety verification of them cannot be ignored. Many researches on MOF-based DDSs are limited to cell experiments in the laboratory, and it is far from enough to be used in the complex physiological environment of human body. Therefore, these systems need to be systematically studied *in vivo* in the future, including their routes of administration, stability in physiological mediators, biological distribution, biodegradation, excretion, and clearance levels. Through these extensive and comprehensive studies, there will be more MOF-based theranostic nanosystems well-designed found to be capable of reaching the market and providing a novel generation of theranostic agents that are more suitable for the diagnosis and treatment of cancer with few side effects.

Acknowledgements This work was financially supported by the National Natural Science Foundation of China (Grant Nos. 51773162 and 21204071).

References

[1] He H, Xie H, Chen Y, et al. Global, regional, and national burdens of bladder cancer in 2017: Estimates from the 2017 global burden of disease study. BMC Public Health, 2020, 20(1): 1693

[2] Sung H, Ferlay J, Siegel R L, et al. Global cancer statistics 2020: GLOBOCAN estimates of incidence and mortality worldwide for 36 cancers in 185 countries. CA: A Cancer Journal for Clinicians, 2021, 71(3): 209–249

[3] Zhang M, Ma Y, Wang Z, et al. A CD44-targeting programmable drug delivery system for enhancing and sensitizing chemotherapy to drug-resistant cancer. ACS Applied Materials & Interfaces, 2019, 11(6): 5851–5861

[4] Kumar A, Jaitak V. Natural products as multidrug resistance modulators in cancer. European Journal of Medicinal Chemistry, 2019, 176: 268–291

[5] Obayemi J D, Salifu A A, Eluu S C, et al. LHRH-conjugated drugs as targeted therapeutic agents for the specific targeting and localized treatment of triple negative breast cancer. Scientific Reports, 2020, 10(1): 8212

[6] Mittra I, Pal K, Pancholi N, et al. Prevention of chemotherapy toxicity by agents that neutralize or degrade cell-free chromatin. Annals of Oncology, 2017, 28(9): 2119–2127

[7] Ding Y, Ma Y, Du C, et al. NO-releasing polypeptide nanocomposites reverse cancer multidrug resistance via triple therapies. Acta Biomaterialia, 2021, 123: 335–345

[8] Mi P. Stimuli-responsive nanocarriers for drug delivery, tumor imaging, therapy and theranostics. Theranostics, 2020, 10(10): 4557–4588

[9] Raj S, Khurana S, Choudhari R, et al. Specific targeting cancer cells with nanoparticles and drug delivery in cancer therapy. Seminars in Cancer Biology, 2021, 69: 166–177

[10] Liu H, Jiang W, Wang Q, et al. ROS-sensitive biomimetic nanocarriers modulate tumor hypoxia for synergistic photodynamic chemotherapy. Biomaterials Science, 2019, 7(9): 3706–3716

[11] Pandey A, Kulkarni S, Vincent A P, et al. Hyaluronic acid-drug conjugate modified core–shell MOFs as pH responsive nanoplatform for multimodal therapy of glioblastoma. International Journal of Pharmaceutics, 2020, 588: 119735

[12] Sanfilippo V, Caruso V C L, Cucci L M, et al. Hyaluronan-metal

gold nanoparticle hybrids for targeted tumor cell therapy. International Journal of Molecular Sciences, 2020, 21(9): 3085–3111

[13] Chen J, Ma Y, Du W, et al. Furin-instructed intracellular gold nanoparticle aggregation for tumor photothermal therapy. Advanced Functional Materials, 2020, 30(50): 2001566

[14] Kong M, Huang Y, Yu R, et al. Coordination bonding-based Fe_3O_4@PDA-Zn^{2+}-doxorubicin nanoparticles for tumor chemo-photothermal therapy. Journal of Drug Delivery Science and Technology, 2019, 51: 185–193

[15] Wen W, Wu L, Chen Y, et al. Ultra-small Fe_3O_4 nanoparticles for nuclei targeting drug delivery and photothermal therapy. Journal of Drug Delivery Science and Technology, 2020, 58: 101782

[16] Guan Y, Yang Y, Wang X, et al. Multifunctional Fe_3O_4@SiO_2-CDs magnetic fluorescent nanoparticles as effective carrier of gambogic acid for inhibiting VX2 tumor cells. Journal of Molecular Liquids, 2021, 327: 114783

[17] Huang L, Liu J, Gao F, et al. A dual-responsive, hyaluronic acid targeted drug delivery system based on hollow mesoporous silica nanoparticles for cancer therapy. Journal of Materials Chemistry B: Materials for Biology and Medicine, 2018, 6(28): 4618–4629

[18] Shao M, Chang C, Liu Z, et al. Polydopamine coated hollow mesoporous silica nanoparticles as pH-sensitive nanocarriers for overcoming multidrug resistance. Colloids and Surfaces B: Biointerfaces, 2019, 183: 110427

[19] Chen K, Chang C, Liu Z, et al. Hyaluronic acid targeted and pH-responsive nanocarriers based on hollow mesoporous silica nanoparticles for chemo-photodynamic combination therapy. Colloids and Surfaces B: Biointerfaces, 2020, 194: 111166

[20] Saleem J, Wang L, Chen C. Carbon-based nanomaterials for cancer therapy via targeting tumor microenvironment. Advanced Healthcare Materials, 2018, 7(20): 1800525

[21] Loh K P, Ho D, Chiu G N C, et al. Clinical applications of carbon nanomaterials in diagnostics and therapy. Advanced Materials, 2018, 30(47): 1802368

[22] Jiang B P, Zhou B, Lin Z, et al. Recent advances in carbon nanomaterials for cancer phototherapy. Chemistry, 2019, 25(16): 3993–4004

[23] Zhao S, Cao W, Xing S, et al. Enhancing effects of theanine liposomes as chemotherapeutic agents for tumor therapy. ACS Biomaterials Science & Engineering, 2019, 5(7): 3373–3379

[24] Zhang K, Zhang Y, Meng X, et al. Light-triggered theranostic liposomes for tumor diagnosis and combined photodynamic and hypoxia-activated prodrug therapy. Biomaterials, 2018, 185: 301–309

[25] Yang Y, Liu X, Ma W, et al. Light-activatable liposomes for repetitive on-demand drug release and immunopotentiation in hypoxic tumor therapy. Biomaterials, 2021, 265: 120456

[26] Yang L, Zhang C, Liu J, et al. ICG-conjugated and ^{125}I-labeled polymeric micelles with high biosafety for multimodality imaging-guided photothermal therapy of tumors. Advanced Healthcare Materials, 2020, 9(5): 1901616

[27] Hu C, Zhuang W, Yu T, et al. Multi-stimuli responsive polymeric prodrug micelles for combined chemotherapy and photodynamic therapy. Journal of Materials Chemistry B: Materials for Biology and Medicine, 2020, 8(24): 5267–5279

[28] Zhong S, Chen C, Yang G, et al. Acid-triggered nanoexpansion polymeric micelles for enhanced photodynamic therapy. ACS Applied Materials & Interfaces, 2019, 11(37): 33697–33705

[29] Li X, Zhang Y, Zhi X, et al. Analysis of clinical efficacy of nano-albumin paclitaxel treatment for advanced cell lung cancer. Journal of Nanoscience and Nanotechnology, 2020, 20(10): 6019–6025

[30] Zhou Y, Chang C, Liu Z, et al. Hyaluronic acid-functionalized hollow mesoporous silica nanoparticles as pH-sensitive nano-carriers for cancer chemo-photodynamic therapy. Langmuir, 2021, 37(8): 2619–2628

[31] Zhang L, Shi X, Zhang Z, et al. Porphyrinic zirconium metal-organic frameworks (MOFs) as heterogeneous photocatalysts for PET-RAFT polymerization and stereolithography. Angewandte Chemie International Edition, 2021, 60(10): 5489–5496

[32] Gulcay E, Erucar I. Biocompatible MOFs for storage and separation of O_2: A molecular simulation study. Industrial & Engineering Chemistry Research, 2019, 58(8): 3225–3237

[33] Daglar H, Gulbalkan H C, Avci G, et al. Effect of metal-organic framework (MOF) database selection on the assessment of gas storage and separation potentials of MOFs. Angewandte Chemie International Edition, 2021, 60(14): 7828–7837

[34] Hao M, Qiu M, Yang H, et al. Recent advances on preparation and environmental applications of MOF-derived carbons in catalysis. Science of the Total Environment, 2021, 760: 143333

[35] Neufeld M J, Winter H, Landry M R, et al. Lanthanide metal-organic frameworks for multispectral radioluminescent imaging. ACS Applied Materials & Interfaces, 2020, 12(24): 26943–26954

[36] Gao X, Cui R, Ji G, et al. Size and surface controllable metal-organic frameworks (MOFs) for fluorescence imaging and cancer therapy. Nanoscale, 2018, 10(13): 6205–6211

[37] Kumar P, Anand B, Tsang Y F, et al. Regeneration, degradation, and toxicity effect of MOFs: Opportunities and challenges. Environmental Research, 2019, 176: 108488

[38] Schnabel J, Ettlinger R, Bunzen H. Zn-MOF-74 as pH-responsive drug-delivery system of arsenic trioxide. Chem-NanoMat, 2020, 6(8): 1229–1236

[39] Liu Z, Li T, Han F, et al. A cascade-reaction enabled synergistic cancer starvation/ROS-mediated/chemo-therapy with an enzyme

modified Fe-based MOF. Biomaterials Science, 2019, 7(9): 3683–3692

[40] Xiao Y, Xu M, Lv N, et al. Dual stimuli-responsive metal-organic framework-based nanosystem for synergistic photothermal/pharmacological antibacterial therapy. Acta Biomaterialia, 2021, 122: 291–305

[41] Liang S, Xiao X, Bai L, et al. Conferring Ti-based MOFs with defects for enhanced sonodynamic cancer therapy. Advanced Materials, 2021, 33(18): 2100333

[42] Sun Q, Bi H, Wang Z, et al. Hyaluronic acid-targeted and pH-responsive drug delivery system based on metal-organic frameworks for efficient antitumor therapy. Biomaterials, 2019, 223: 119473

[43] Jiang Z, Wang T, Yuan S, et al. A tumor-sensitive biological metal-organic complex for drug delivery and cancer therapy. Journal of Materials Chemistry B: Materials for Biology and Medicine, 2020, 8(32): 7189–7196

[44] Pan W, Shi M, Li Y, et al. A GSH-responsive nanophotosensitizer for efficient photodynamic therapy. RSC Advances, 2018, 8 (74): 42374–42379

[45] Yu L Y, Shen Y A, Chen M H, et al. The feasibility of ROS- and GSH-responsive micelles for treating tumor-initiating and metastatic cancer stem cells. Journal of Materials Chemistry B: Materials for Biology and Medicine, 2019, 7(19): 3109–3118

[46] Sameiyan E, Bagheri E, Dehghani S, et al. Aptamer-based ATP-responsive delivery systems for cancer diagnosis and treatment. Acta Biomaterialia, 2021, 123: 110–122

[47] Yuwen L, Qiu Q, Xiu W, et al. Hyaluronidase-responsive phototheranostic nanoagents for fluorescence imaging and photothermal/photodynamic therapy of methicillin-resistant *Staphylococcus aureus* infections. Biomaterials Science, 2021, 9 (12): 4484–4495

[48] Zhang N, Li M, Sun X, et al. NIR-responsive cancer cytomembrane-cloaked carrier-free nanosystems for highly efficient and self-targeted tumor drug delivery. Biomaterials, 2018, 159: 25–36

[49] Ding Y, Du C, Qian J, et al. NIR-responsive polypeptide nanocomposite generates NO gas, mild photothermia, and chemotherapy to reverse multidrug-resistant cancer. Nano Letters, 2019, 19(7): 4362–4370

[50] Zhang W, Lu J, Gao X, et al. Enhanced photodynamic therapy by reduced levels of intracellular glutathione obtained by employing a nano-MOF with Cu(II) as the active center. Angewandte Chemie International Edition, 2018, 57(18): 4891–4896

[51] Sabz M, Kamali R, Ahmadizade S. Numerical simulation of magnetic drug targeting to a tumor in the simplified model of the human lung. Computer Methods and Programs in Biomedicine, 2019, 172: 11–24

[52] Shen S, Huang D, Cao J, et al. Magnetic liposomes for light-sensitive drug delivery and combined photothermal-chemotherapy of tumors. Journal of Materials Chemistry B: Materials for Biology and Medicine, 2019, 7(7): 1096–1106

[53] Nguyen Cao T G, Kang J H, You J Y, et al. Safe and targeted sonodynamic cancer therapy using biocompatible exosome-based nanosonosensitizers. ACS Applied Materials & Interfaces, 2021, 13(22): 25575–25588

[54] Mathesh M, Sun J, van der Sandt F, et al. Supramolecular nanomotors with “pH taxis” for active drug delivery in the tumor microenvironment. Nanoscale, 2020, 12(44): 22495–22501

[55] Yan T, Zhu S, Hui W, et al. Chitosan based pH-responsive polymeric prodrug vector for enhanced tumor targeted co-delivery of doxorubicin and siRNA. Carbohydrate Polymers, 2020, 250: 116781

[56] Lázaro I A, Haddad S, Sacca S, et al. Selective surface PEGylation of UiO-66 nanoparticles for enhanced stability, cell uptake, and pH-responsive drug delivery. Chem, 2017, 2(4): 561–578

[57] Jiang K, Zhang L, Hu Q, et al. Indocyanine green-encapsulated nanoscale metal-organic frameworks for highly effective chemo-photothermal combination cancer therapy. Materials Today Nano, 2018, 2: 50–57

[58] Yu S, Wang S, Xie Z, et al. Hyaluronic acid coating on the surface of curcumin-loaded ZIF-8 nanoparticles for improved breast cancer therapy: An *in vitro* and *in vivo* study. Colloids and Surfaces B: Biointerfaces, 2021, 203: 111759

[59] Qin Y T, Peng H, He X W, et al. pH-responsive polymer-stabilized ZIF-8 nanocomposites for fluorescence and magnetic resonance dual-modal imaging-guided chemo-/photodynamic combinational cancer therapy. ACS Applied Materials & Interfaces, 2019, 11(37): 34268–34281

[60] Zhu J, Li H, Xiong Z, et al. Polyethyleneimine-coated manganese oxide nanoparticles for targeted tumor PET/MR imaging. ACS Applied Materials & Interfaces, 2018, 10(41): 34954–34964

[61] Liu Z, Shen N, Tang Z, et al. An eximious and affordable GSH stimulus-responsive poly(α-lipoic acid) nanocarrier bonding combretastatin A4 for tumor therapy. Biomaterials Science, 2019, 7(7): 2803–2811

[62] Lin C, He H, Zhang Y, et al. Acetaldehyde-modified-cystine functionalized Zr-MOFs for pH/GSH dual-responsive drug delivery and selective visualization of GSH in living cells. RSC Advances, 2020, 10(6): 3084–3091

[63] Li J, Wang Y, Sun S, et al. Disulfide bond-based self-crosslinked carbon-dots for turn-on fluorescence imaging of GSH in living cells. The Analyst, 2020, 145(8): 2982–2987

[64] Lei B, Wang M, Jiang Z, et al. Constructing redox-responsive metal-organic framework nanocarriers for anticancer drug

delivery. ACS Applied Materials & Interfaces, 2018, 10(19): 16698–16706

[65] Liu Y, Gong C S, Dai Y, et al. *In situ* polymerization on nanoscale metal-organic frameworks for enhanced physiological stability and stimulus-responsive intracellular drug delivery. Biomaterials, 2019, 218: 119365–119375

[66] Deng J, Wang K, Wang M, et al. Mitochondria targeted nanoscale zeolitic imidazole framework-90 for ATP imaging in live cells. Journal of the American Chemical Society, 2017, 139(16): 5877–5882

[67] Song X R, Li S H, Dai J, et al. Polyphenol-inspired facile construction of smart assemblies for ATP- and pH-responsive tumor MR/Optical imaging and photothermal therapy. Small, 2017, 13(20): 1603997

[68] Chen W H, Yu X, Cecconello A, et al. Stimuli-responsive nucleic acid-functionalized metal-organic framework nanoparticles using pH- and metal-ion-dependent DNAzymes as locks. Chemical Science, 2017, 8(8): 5769–5780

[69] Chen W H, Liao W C, Sohn Y S, et al. Stimuli-responsive nucleic acid-based polyacrylamide hydrogel-coated metal-organic framework nanoparticles for controlled drug release. Advanced Functional Materials, 2018, 28(8): 1705137

[70] Wan S S, Zhang L, Zhang X Z. An ATP-regulated ion transport nanosystem for homeostatic perturbation therapy and sensitizing photodynamic therapy by autophagy inhibition of tumors. ACS Central Science, 2019, 5(2): 327–340

[71] Zuo W, Chen D, Fan Z, et al. Design of light/ROS cascade-responsive tumor-recognizing nanotheranostics for spatiotemporally controlled drug release in locoregional photo-chemotherapy. Acta Biomaterialia, 2020, 111: 327–340

[72] Lv W, Xia H, Zou L, et al. Yolk–shell structured Au nanorods@mesoporous silica for gas bubble driven drug release upon near-infrared light irradiation. Nanomedicine: Nanotechnology, Biology, and Medicine, 2021, 32: 102326

[73] Zhu X, Su Q, Feng W, et al. Anti-Stokes shift luminescent materials for bio-applications. Chemical Society Reviews, 2017, 46(4): 1025–1039

[74] Xu J, Gulzar A, Liu Y, et al. Integration of IR-808 sensitized upconversion nanostructure and MoS_2 nanosheet for 808 nm NIR light triggered phototherapy and bioimaging. Small, 2017, 13(36): 17018141

[75] Lismont M, Dreesen L, Wuttke S. Metal-organic framework nanoparticles in photodynamic therapy: Current status and perspectives. Advanced Functional Materials, 2017, 27(14): 1606314

[76] Park J, Jiang Q, Feng D, et al. Size-controlled synthesis of porphyrinic metal-organic framework and functionalization for targeted photodynamic therapy. Journal of the American Chemical Society, 2016, 138(10): 3518–3525

[77] Liu J, Yang Y, Zhu W, et al. Nanoscale metal-organic frameworks for combined photodynamic & radiation therapy in cancer treatment. Biomaterials, 2016, 97: 1–9

[78] Li B, Wang X, Chen L, et al. Ultrathin Cu-TCPP MOF nanosheets: A new theragnostic nanoplatform with magnetic resonance/near-infrared thermal imaging for synergistic phototherapy of cancers. Theranostics, 2018, 8(15): 4086–4096

[79] Wang Y, Shi L, Ma D, et al. Tumor-activated and metal-organic framework assisted self-assembly of organic photosensitizers. ACS Nano, 2020, 14(10): 13056–13068

[80] Yang D, Xu J, Yang G, et al. Metal-organic frameworks join hands to create an anti-cancer nanoplatform based on 808 nm light driving up-conversion nanoparticles. Chemical Engineering Journal, 2018, 344: 363–374

[81] Huang J, Xu Z, Jiang Y, et al. Metal organic framework-coated gold nanorod as an on-demand drug delivery platform for chemo-photothermal cancer therapy. Journal of Nanobiotechnology, 2021, 19(1): 219

[82] Cai X, Xie Z, Ding B, et al. Monodispersed copper(I)-based nano metal-organic framework as a biodegradable drug carrier with enhanced photodynamic therapy efficacy. Advanced Science, 2019, 6(15): 1900848

[83] Cai X, Jiang Y, Lin M, et al. Ultrasound-responsive materials for drug/gene delivery. Frontiers in Pharmacology, 2020, 10: 1650

[84] Cui X, Han X, Yu L, et al. Intrinsic chemistry and design principle of ultrasound-responsive nanomedicine. Nano Today, 2019, 28: 100773

[85] Ibrahim M, Sabouni R, Husseini G A, et al. Facile ultrasound-triggered release of calcein and doxorubicin from iron-based metal-organic frameworks. Journal of Biomedical Nanotechnology, 2020, 16(9): 1359–1369

[86] Zhou Y, Wang M, Dai Z. The molecular design of and challenges relating to sensitizers for cancer sonodynamic therapy. Materials Chemistry Frontiers, 2020, 4(8): 2223–2234

[87] Huang C, Ding S, Jiang W, et al. Glutathione-depleting nanoplatelets for enhanced sonodynamic cancer therapy. Nanoscale, 2021, 13(8): 4512–4518

[88] Pan X, Wang W, Huang Z, et al. MOF-derived double-layer hollow nanoparticles with oxygen generation ability for multimodal imaging-guided sonodynamic therapy. Angewandte Chemie International Edition, 2020, 59(32): 13557–13561

[89] Ke X, Song X, Qin N, et al. Rational synthesis of magnetic Fe_3O_4@MOF nanoparticles for sustained drug delivery. Journal of Porous Materials, 2019, 26(3): 813–818

[90] Aghayi-Anaraki M, Safarifard V. Fe_3O_4@MOF magnetic nanocomposites: Synthesis and applications. European Journal of Inorganic Chemistry, 2020, 2020(20): 1916–1937

[91] Xiang Z, Qi Y, Lu Y, et al. MOF-derived novel porous Fe_3O_4@C nanocomposites as smart nanomedical platforms for combined cancer therapy: Magnetic-triggered synergistic hyperthermia and chemotherapy. Journal of Materials Chemistry B: Materials for Biology and Medicine, 2020, 8(37): 8671–8683

[92] Lin R, Yu W, Chen X, et al. Self-propelled micro/nanomotors for tumor targeting delivery and therapy. Advanced Healthcare Materials, 2021, 10(1): 2001212

[93] Xu J, Lee S S, Seo H, et al. Quinic acid-conjugated nanoparticles enhance drug delivery to solid tumors via interactions with endothelial selectins. Small, 2018, 14(50): 1803601

[94] Park J, Choi Y, Chang H, et al. Alliance with EPR effect: Combined strategies to improve the EPR effect in the tumor microenvironment. Theranostics, 2019, 9(26): 8073–8090

[95] Xue T, Xu C, Wang Y, et al. Doxorubicin-loaded nanoscale metal-organic framework for tumor-targeting combined chemotherapy and chemodynamic therapy. Biomaterials Science, 2019, 7(11): 4615–4623

[96] Liu P, Zhou Y, Shi X, et al. A cyclic nano-reactor achieving enhanced photodynamic tumor therapy by reversing multiple resistances. Journal of Nanobiotechnology, 2021, 19(1): 149

[97] Yan J, Liu C, Wu Q, et al. Mineralization of pH-sensitive doxorubicin prodrug in ZIF-8 to enable targeted delivery to solid tumors. Analytical Chemistry, 2020, 92(16): 11453–11461

[98] Xu W, Lou Y, Chen W, et al. Folic acid decorated metal-organic frameworks loaded with doxorubicin for tumor-targeted chemotherapy of osteosarcoma. Biomedical Engineerin/Biomedizinische Technik, 2020, 65(2): 229–236

[99] Samui A, Pal K, Karmakar P, et al. *In situ* synthesized lactobionic acid conjugated NMOFs, a smart material for imaging and targeted drug delivery in hepatocellular carcinoma. Materials Science and Engineering C, 2019, 98: 772–781

[100] Zhang H, Zhang Q, Liu C, et al. Preparation of a one-dimensional nanorod/metal organic framework Janus nanoplatform via side-specific growth for synergistic cancer therapy. Biomaterials Science, 2019, 7(4): 1696–1704

[101] He Y, Xiong T, He S, et al. Pulmonary targeting crosslinked cyclodextrin metal-organic frameworks for lung cancer therapy. Advanced Functional Materials, 2021, 31(3): 2004550

[102] Zhang Y, Lin L, Liu L, et al. Positive feedback nanoamplifier responded to tumor microenvironments for self-enhanced tumor imaging and therapy. Biomaterials, 2019, 216: 119255–119263

[103] Kim K, Lee S, Jin E, et al. MOF × biopolymer: Collaborative combination of metal-organic framework and biopolymer for advanced anticancer therapy. ACS Applied Materials & Interfaces, 2019, 11(31): 27512–27520

[104] Wu M, Liu X, Bai H, et al. Surface-layer protein-enhanced immunotherapy based on cell membrane-coated nanoparticles for the effective inhibition of tumor growth and metastasis. ACS Applied Materials & Interfaces, 2019, 11(10): 9850–9859

[105] Chai Z, Hu X, Lu W. Cell membrane-coated nanoparticles for tumor-targeted drug delivery. Science China Materials, 2017, 60(6): 504–510

[106] Wan X, Song L, Pan W, et al. Tumor-targeted cascade nanoreactor based on metal-organic frameworks for synergistic ferroptosis-starvation anticancer therapy. ACS Nano, 2020, 14(9): 11017–11028

[107] Owens E A, Henary M, El Fakhri G, et al. Tissue-specific near-infrared fluorescence imaging. Accounts of Chemical Research, 2016, 49(9): 1731–1740

[108] Liu J, Liu Z, Wu D. Multifunctional hypoxia imaging nanoparticles: multifunctional tumor imaging and related guided tumor therapy. International Journal of Nanomedicine, 2019, 14: 707–719

[109] Sun J, Wang J, Hu W, et al. Camouflaged gold nanodendrites enable synergistic photodynamic therapy and NIR biowindow II photothermal therapy and multimodal imaging. ACS Applied Materials & Interfaces, 2021, 13(9): 10778–10795

[110] Ouyang Z, Li D, Xiong Z, et al. Antifouling dendrimer-entrapped copper sulfide nanoparticles enable photoacoustic imaging-guided targeted combination therapy of tumors and tumor metastasis. ACS Applied Materials & Interfaces, 2021, 13(5): 6069–6080

[111] Zhou G, Wang Y S, Jin Z, et al. Porphyrin-palladium hydride MOF nanoparticles for tumor-targeting photoacoustic imaging-guided hydrogenothermal cancer therapy. Nanoscale Horizons, 2019, 4(5): 1185–1193

[112] Wang Y, Wu W, Mao D, et al. Metal-organic framework assisted and tumor microenvironment modulated synergistic image-guided photo-chemo therapy. Advanced Functional Materials, 2020, 30(28): 2002431

[113] Chen Y, Li Z H, Pan P, et al. Tumor-microenvironment-triggered ion exchange of a metal-organic framework hybrid for multimodal imaging and synergistic therapy of tumors. Advanced Materials, 2020, 32(24): 2001452

[114] Peller M, Böll K, Zimpel A, et al. Metal-organic framework nanoparticles for magnetic resonance imaging. Inorganic Chemistry Frontiers, 2018, 5(8): 1760–1779

[115] McLeod S M, Robison L, Parigi G, et al. Maximizing magnetic resonance contrast in Gd(III) nanoconjugates: Investigation of proton relaxation in zirconium metal-organic frameworks. ACS Applied Materials & Interfaces, 2020, 12(37): 41157–41166

[116] Yao J, Liu Y, Wang J, et al. On-demand CO release for amplification of chemotherapy by MOF functionalized magnetic carbon nanoparticles with NIR irradiation. Biomaterials, 2019, 195: 51–62

[117] Ebrahimpour A, Riahi Alam N, Abdolmaleki P, et al. Magnetic metal-organic framework based on zinc and 5-aminolevulinic acid: MR imaging and brain tumor therapy. Journal of Inorganic and Organometallic Polymers and Materials, 2021, 31(3): 1208–1216

[118] Zhou H, Qi M, Shao J, et al. Manganese oxide/metal-organic frameworks-based nanocomposites for tumr micro-environment sensitive $^{1}H/^{19}F$ dual-mode magnetic resonance imaging *in vivo*. Journal of Organometallic Chemistry, 2021, 933: 121652

[119] Guo C, Xu S, Arshad A, et al. A pH-responsive nanoprobe for turn-on ^{19}F-magnetic resonance imaging. Chemical Communications, 2018, 54(70): 9853–9856

[120] Zhu W, Chen M, Liu Y, et al. A dual factor activated metal-organic framework hybrid nanoplatform for photoacoustic imaging and synergetic photo-chemotherapy. Nanoscale, 2019, 11(43): 20630–20637

[121] Pu Y, Zhu Y, Qiao Z, et al. A Gd-doped polydopamine (PDA)-based theranostic nanoplatform as a strong MR/PA dual-modal imaging agent for PTT/PDT synergistic therapy. Journal of Materials Chemistry B: Materials for Biology and Medicine, 2021, 9(7): 1846–1857

[122] Wan S S, Cheng Q, Zeng X, et al. A Mn(III)-sealed metal-organic framework nanosystem for redox-unlocked tumor theranostics. ACS Nano, 2019, 13(6): 6561–6571

[123] Zhu Y, Xin N, Qiao Z, et al. Bioactive MOFs based theranostic agent for highly effective combination of multimodal imaging and chemo-phototherapy. Advanced Healthcare Materials, 2020, 9(14): 2000205

[124] Cai W, Gao H, Chu C, et al. Engineering phototheranostic nanoscale metal-organic frameworks for multimodal imaging-guided cancer therapy. ACS Applied Materials & Interfaces, 2017, 9(3): 2040–2051

[125] Sun X, He G, Xiong C, et al. One-pot fabrication of hollow porphyrinic MOF nanoparticles with ultrahigh drug loading toward controlled delivery and synergistic cancer therapy. ACS Applied Materials & Interfaces, 2021, 13(3): 3679–3693